

Nanoindentation of $\text{Si}_{1-x}\text{Ge}_x$ thin films prepared by biased target ion beam deposition

Ruijing Ge^{1,2}, Xiaowei Hou^{1,3}, Kirsten Brookshire¹, N. Radha Krishnan¹, Dilusha Silva¹, John Bumgarner¹, Yinong Liu⁴, Lorenzo Faraone¹, Mariusz Martyniuk¹

¹School of Electrical, Electronic and Computer Engineering, The University of Western Australia, 35 Stirling Highway, Crawley, WA, Australia 6009

²School of The Gifted Young, University of Science and Technology of China, Anhui, 230026, China

³School of Electronics and Information, Northwestern Polytechnical University, Xi'an 710072, China

⁴School of Mechanical and Chemical Engineering, The University of Western Australia, 35 Stirling Highway, Crawley, WA, Australia 6009

Abstract—The mechanical properties of $\text{Si}_{1-x}\text{Ge}_x$ thin films are studied via nanoindentation. The $\text{Si}_{1-x}\text{Ge}_x$ thin films are prepared with a biased target ion beam deposition (BTIBD) method. We investigate the effect of varying the Si to Ge composition ratio on the elastic modulus and hardness of the resulting alloyed films. In comparison to pure BTIBD Si ($E_{\text{Si}} = 154\text{GPa}$, $H_{\text{Si}} = 9.9\text{GPa}$), for $\text{Si}_{1-x}\text{Ge}_x$ a decreasing trend in Young's modulus and hardness is observed to be associated with the increase in Ge content, and for $\text{Si}_{0.5}\text{Ge}_{0.5}$ the values of 139 GPa and 8.4GPa are found to represent the Young's modulus and hardness, respectively.

Index Terms—amorphous silicon, BTIBD, germanium, hardness, nanoindentation, young's modulus

I. INTRODUCTION

Si and Ge are two thin film materials frequently used in electron transport devices. Incorporation of Ge with Si to form the $\text{Si}_{1-x}\text{Ge}_x$ alloy has found applications as a novel high-speed Si-system material with the aim to improve the electron and hole carrier mobilities for many devices such as metal-oxide semiconductor field effect transistors (MOSFETs), modulation-doped field effect transistors (MODFETs), and doped-channel field effect transistors (DCFETs). $\text{Si}_{1-x}\text{Ge}_x/\text{Si}_{1-y}\text{Ge}_y$ hetero-structures are also used in quantum effect devices such as resonant-tunneling diodes (RTDs), which show the potential to become the next-generation high-speed Si-system devices. However, application of this material system towards micro-electro-mechanical systems (MEMS) has received little attention. This is desirable since varying the Si to Ge composition ratio allows for controlling the thin film stress, which is a very important aspect for MEMS. For such applications, it is essential to grow high quality $\text{Si}_{1-x}\text{Ge}_x$ thin films and have a good understanding of their fundamental mechanical properties, such as Young's modulus and hardness.

A variety of methods have been used to deposit thin films, such as vacuum evaporation [1-2], magnetron sputtering [3-4], ion beam deposition [5-8], chemical vapour deposition (CVD) [9], and molecular beam epitaxy (MBE) [10]. Among these methods, ion beam deposition is widely used.

Mechanical properties of materials significantly influence device robustness and stability and are very important for device operation. Instrumented nanoindentation is a simple technique that can be used to study quantitatively the basic mechanical properties of thin films grown on substrates, such as elastic modulus and hardness [11-15]. In this paper, we present a study of the fundamental mechanical properties of SiGe thin films deposited using BTIBD [16]. Nanoindentation technique is used to study the elastic modulus and hardness of the SiGe thin films as a function of relative Si and Ge content.

II. EXPERIMENTAL

Elemental sputtering targets of pure Si and Ge were used as source material for film deposition. The targets were 4" in diameter and 6 mm in thickness. Films were deposited on to 300 μm -thick, Si <100> p-type wafers. All substrates were cleaned ultrasonically in subsequent baths of acetone, methanol and isopropanol. The sputtering and base pressures were maintained at 4.8×10^{-4} Torr and 8.0×10^{-8} Torr, respectively. The Si to Ge composition ratio was controlled via sputtering rates from individual targets that were controlled via target bias duty cycles as described previously in Ref. [17]. The thickness of all deposited films was 500nm.

The Young's modulus and hardness of thin films were determined using nanoindentation technique, which were conducted by a Hysitron TriboScope (Hysitron, Minneapolis, MN) nanomechanical testing instrument using a Berkovich indenter tip. The diamond Berkovich tip had a radius of ~ 100 nm. For each specimen, over 30 indents were performed at loads ranging from 500 μN to 10,000 μN . Determinations of elastic modulus and hardness were made from the load-displacement (P-h) curves according to the Oliver and Pharr method [12] over indenter penetration depths ranging from 50 to 240 nm.

III. RESULTS AND DISCUSSIONS

Figures 1 (a), (b) and (c) show sample load-displacement curves of silicon, $\text{Si}_{0.5}\text{Ge}_{0.5}$ and germanium thin films on Si substrates, respectively. It can be observed in Fig. 1, that for Si and $\text{Si}_{0.5}\text{Ge}_{0.5}$ the successively deeper indentation curves

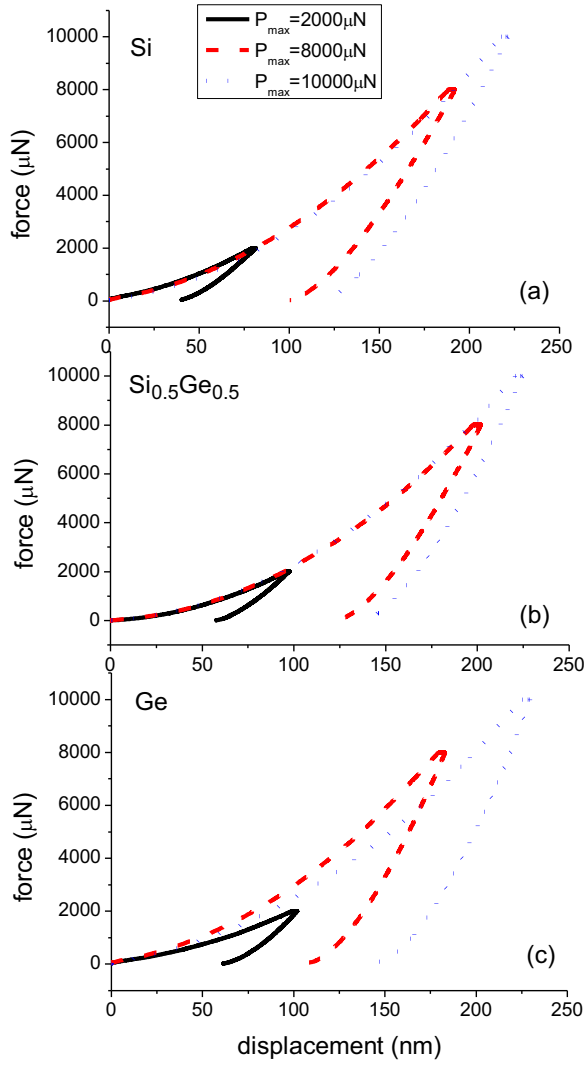


Fig. 1. Nanoindentation load-displacement curves for BTIBD (a) Si, (b) $\text{Si}_{0.5}\text{Ge}_{0.5}$ and (c) Ge thin films.

overlay each other very well. We present sample curves in Fig. 1, however, we have observed this behavior for all the curves for both Si and $\text{Si}_{0.5}\text{Ge}_{0.5}$ materials as well as for $\text{Si}_{0.6}\text{Ge}_{0.4}$, $\text{Si}_{0.7}\text{Ge}_{0.3}$, $\text{Si}_{0.8}\text{Ge}_{0.2}$, and $\text{Si}_{0.9}\text{Ge}_{0.1}$ thin films. This indicates repeatability and material uniformity. However, the P-h curves for pure germanium thin film (see Fig. 1(c)) do exhibit significant scatter.

The reduced modulus measured during nanoindentation, E_r , is a factor of both the film and the indenter tip. It is given by

$$\frac{1}{E_r} = \left(\frac{1 - \nu^2}{E} \right)_{\text{sample}} + \left(\frac{1 - \nu_i^2}{E_i} \right)_{\text{indenter}}$$

From E_r we can calculate the Young's modulus, E , for our thin film and it is influenced by the value of the Poisson ratio, ν , adopted for the sample. During calculations we used the following values [18]

$$\nu_{\text{silicon}} = 0.28, \quad \nu_i = 0.07, \quad E_i = 1140 \text{ GPa}$$

and the calculated E values for Si, $\text{Si}_{0.5}\text{Ge}_{0.5}$, and Ge thin films are plotted as a function of the contact depth in Fig. 2.

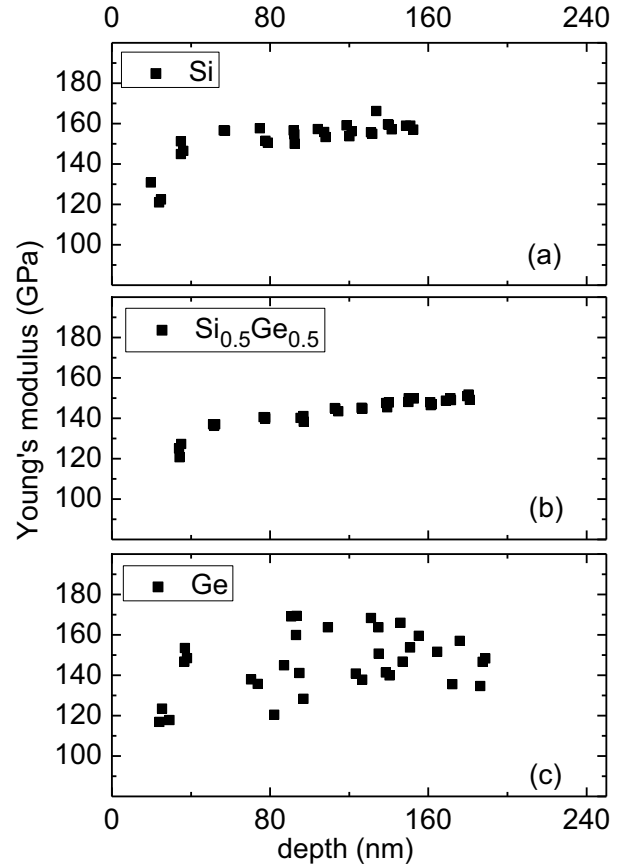


Fig. 2. Young's modulus as a function of the contact depth for BTIBD (a) Si, (b) $\text{Si}_{0.5}\text{Ge}_{0.5}$, and (c) Ge thin films on silicon substrates.

Common trends in the data shown in Fig. 2(a) and Fig. 2(b) can be observed. We note that there is an abrupt decrease of Young's modulus values as the contact depth decreases below 50nm. We attribute this to the limitations of the measurement technique associated with the non-idealities in the tip area function used in the analysis and do not use the data in the contact depth range from 0 to 50nm in further analysis and discussion. We also observe that the values of Young's modulus for indentations exceeding 100nm show an increasing trend with increasing contact depth. We attribute this to the influence of Si substrate. The Young's modulus value associated with the plateau observed in the contact depth range between 50 and 100nm is taken to be the value representative of the thin film properties. We found these above described trends common to all data obtained for Si and $\text{Si}_{0.5}\text{Ge}_{0.5}$, as well as for $\text{Si}_{0.6}\text{Ge}_{0.4}$, $\text{Si}_{0.7}\text{Ge}_{0.3}$, $\text{Si}_{0.8}\text{Ge}_{0.2}$, and $\text{Si}_{0.9}\text{Ge}_{0.1}$ thin films. The experimentally observed Young's modulus and hardness for our Si substrates were 167GPa and 10.9GPa, respectively.

However, as seen in Fig. 2(c) the values of Young's modulus obtained for pure germanium thin films exhibit significant scatter as a function of contact depth. This could be representative of factors associated with material non-uniformities and/or surface roughness and is the topic of subsequent investigations.

The correlation of values obtained for thin film hardness with contact depth is shown in Fig. 3 for Si, $\text{Si}_{0.5}\text{Ge}_{0.5}$, and

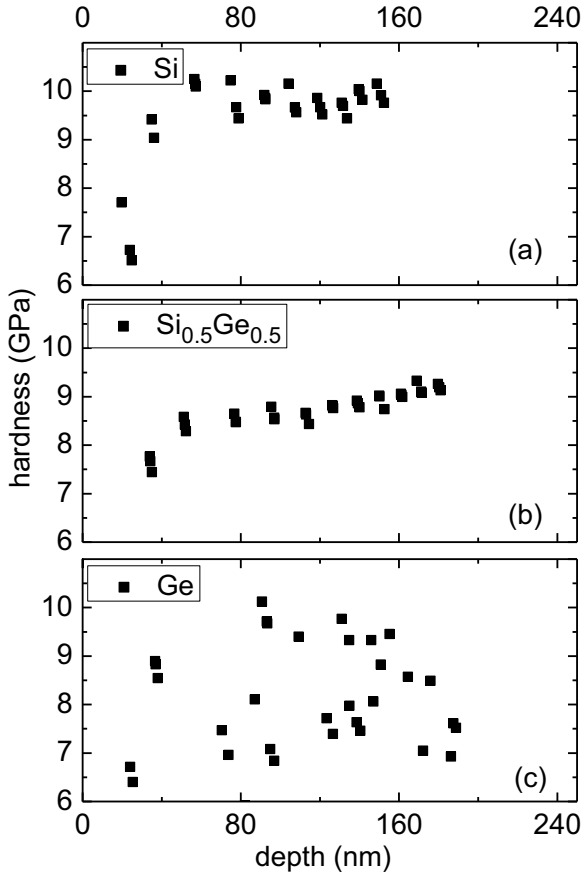


Fig. 3. Hardness as a function of the contact depth for BTIBD (a) Si, (b) $\text{Si}_{0.5}\text{Ge}_{0.5}$, and (c) Ge thin films on silicon substrates.

Ge. We observe similar trends as in the case of the correlation of values for Young's modulus with contact depth. Below 50nm the data is impacted by the limitations of the tip area function, and as the contact depth increases beyond 100 nm the hardness values increase due to the influence of Si substrate. We found this to be common to all data obtained for Si, $\text{Si}_{0.5}\text{Ge}_{0.5}$, $\text{Si}_{0.6}\text{Ge}_{0.4}$, $\text{Si}_{0.7}\text{Ge}_{0.3}$, $\text{Si}_{0.8}\text{Ge}_{0.2}$, and $\text{Si}_{0.9}\text{Ge}_{0.1}$ thin films. As in the case of the Young's modulus the hardness value associated with the plateau observed in the contact depth range between 50 and 100nm is taken to be the value representative of the thin film properties.

Similarly as it was observed for Young's modulus values obtained for Ge, the hardness values obtained for Ge (see Fig. 3(c)) also exhibit significant scatter as a function of contact depth. The averaged value for measurements in contact depth range between 50nm and 100nm is taken as representative of the Ge film properties.

Fig. 4(a) and Fig. 4(b) show the Young's modulus and hardness, respectively, as a function of percentage of Si content in the investigated $\text{Si}_{1-x}\text{Ge}_x$ thin films. Since the data for Ge presented in Fig. 2(c) and Fig. 3(c) show significant scatter the points in Fig. 4 associated with Ge have significantly greater error bars in comparison to points associated with other compositions, where standard deviations are typically less than 3%. A common trend as a function of film composition for both Young's modulus and

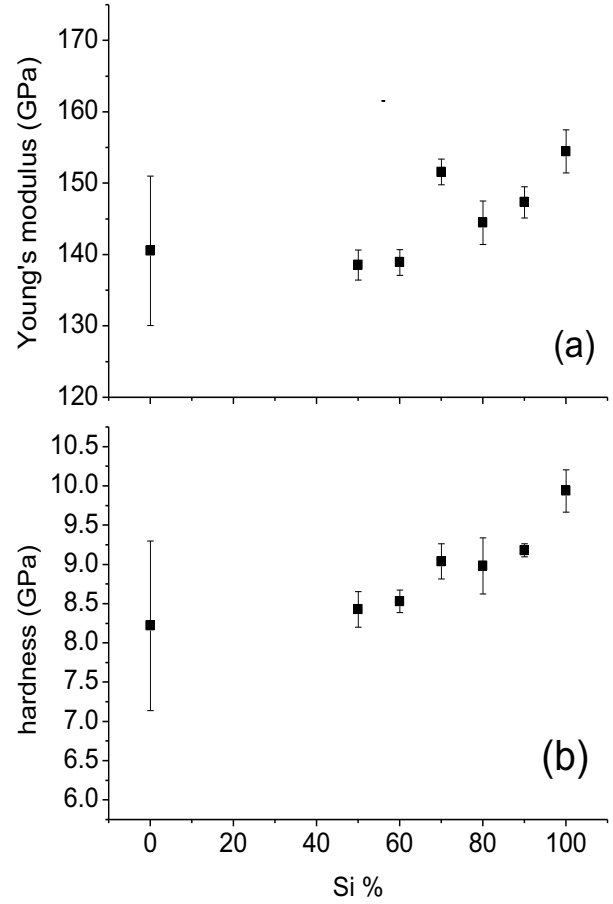


Fig. 4. The correlation of (a) Young's modulus, and (b) hardness with the percentage of silicon within the BTIBD $\text{Si}_{1-x}\text{Ge}_x$ films

hardness can be observed in Fig. 4. It is found that Si thin films prepared using BTIB are characterized by Young's modulus and hardness values of $E = 154\text{GPa}$ and $H = 9.9\text{GPa}$, respectively; which is respectively 92% and 91% of the Young's modulus and hardness values found for (100) single crystalline Si substrates. In comparison to pure BTIBD Si, the values of Young's modulus and hardness obtained for $\text{Si}_{1-x}\text{Ge}_x$ exhibit a decreasing trend with the increase in Ge content. The values for Young's modulus and hardness for $\text{Si}_{0.5}\text{Ge}_{0.5}$ have been found to be 139GPa , and 8.4GPa , respectively. Alloys of $\text{Si}_{1-x}\text{Ge}_x$ with Ge content below 50% were not prepared and not subject to current investigation (apart from pure Ge).

IV. CONCLUSIONS

The mechanical properties of $\text{Si}_{1-x}\text{Ge}_x$ thin films prepared using BTIBD were studied via nanoindentation as a function of thin film Si to Ge relative content. It is found that Si thin films prepared using BTIBD are characterized by Young's modulus and hardness values that are below the values for bulk silicon, and amount respectively to 92% and 91% of the Young's modulus and hardness values found for (100) single crystalline Si substrates. In comparison to pure BTIBD Si ($E_{\text{Si}} = 154\text{GPa}$, $H_{\text{Si}} = 9.9\text{GPa}$), the values of Young's modulus and hardness obtained for $\text{Si}_{1-x}\text{Ge}_x$ exhibit a decreasing trend with the increase in Ge content. It was

observed that in comparison to other compositions studied, the nanoindentation data obtained for pure germanium are significantly scattered. This could be representative of factors associated with surface roughness and/or material non-uniformities.

ACKNOWLEDGMENT

We acknowledge the support from the Australian Research Council, Western Australian Node of the Australian National Fabrication Facility, Centre for Microscopy, Characterisation and Analysis (CMCA) at the University of Western Australia (UWA), and the Office of Science of the WA State Government.

REFERENCES

- [1] Y. Saito, "Crystal structure and habit of silicon and germanium particles grown in argon gas," *Journal of Crystal Growth*, vol. 47, pp. 61-72, 1979.
- [2] R. N. Kr  l, M. L. Mouss  , Y. Tch      , F. X. D. Bouo Bella, B. Aka, and P. A. Thomas, "Optical absorption of the hydrogenated evaporated amorphous silicon," *International Journal of Physical Sciences*, vol. 5, pp. 675-682, 2010.
- [3] P. Reinig, V. Alex, F. Fenske, W. Fuhs, and B. Selle, "Pulsed dc magnetron-sputtering of microcrystalline silicon," *Thin Solid Films*, vol. 403, pp. 86-90, 2002.
- [4] A. Fedala, R. Cherfi, M. Aoucher, and T. Mohammed-Brahim, "Structural, optical and electrical properties of hydrogenated amorphous silicon germanium (a-Si1-xGex) deposited by DC magnetron sputtering at high rate," *Materials Science in Semiconductor Processing*, vol. 9, pp. 690-693, 2006.
- [5] L.N.Aleksandrov, R.N. Lovyagin, O.P. Pchelyakov, and S.I. Stenin, "Heteroepitaxy of germanium thin films on silicon by ion sputtering," *Journal of Crystal Growth*, vol. 24, pp. 298-301, 1974.
- [6] Kunihiro Yagi, Shozo Tamura, and Takashi Tokuyama, "Germanium and Silicon Film Growth by Low-Energy Ion Beam Deposition," *Japanese Journal of Applied Physics*, vol. 16, pp. 245-251, 1977.
- [7] Junji Saraie, Michiya Kobayashi, Yoshishisa Fujii, and Hiroyuki Matsunami, "Preparation of hydrogenated amorphous silicon films by ion beam sputtering," *Thin Solid Films*, vol. 80, pp. 169-176, 1981.
- [8] Kiyoshi Miyake and Takashi Tokuyama, "Germanium and silicon ion beam deposition," *Thin Solid Films*, vol. 92, pp. 123-129, 1982.
- [9] S. Miyazaki, H. Takahashi, H. Yamashita, M. Narasaki, and M. Hirose, "Growth and characterization of microcrystalline silicon-germanium films," *Journal of Non-Crystalline Solids*, vol. 29, pp. 148-152, 2002.
- [10] O.P. Pchelyakov, Y.B. Bolkhovityanov, A.V. Dvurechenskii, A.I. Nikiforov, A.I. Yakimov, and B. Voigtl  nder, "Molecular beam epitaxy of silicon-germanium nanostructures," *Thin Solid Films*, vol. 367, pp. 75-84, 2000.
- [11] A.K. Bhattacharya, W.D. Nix, *Int. J. Solids Struct.* 24 (1988) 1287.
- [12] W.C. Oliver, G.M. Pharr, *J. Mater. Res.* 19 (2004) 3.
- [13] X.Z. Hu, B.R. Lawn, *Thin Solids Films* 322 (1998) 225.
- [14] Y.-G. Jung, B.R. Lawn, M. Martyniuk, H. Huang, X.Z. Hu, *J. Mater. Res.* 19 (2004) 3076.
- [15] Martyniuk, M., Musca, C.A., Dell, J.M., Elliman, R.G., Faraone, L., Elasto-plastic characterisation of low-temperature plasma-deposited silicon nitride thin films using nanoindentation, *International Journal of Surface Science and Engineering* 3 (1-2), pp. 3-22, 2009
- [16] H. N. G. Wadley, X. W. Zhou, and J. J. Quan, "Biased Target Ion Beam Deposition of GMR Multilayers," *Proceedings of Non-volatile Memory Technology Symposium*, 2003, pp. 12-1.
- [17] Krishnan, N.R., Martyniuk, M., Jeffery, R.D., (...), Dell, J.M., Faraone, L., Control of chemical composition of rare-earth substituted iron garnets using biased target deposition, *Conference on Optoelectronic and Microelectronic Materials and Devices*, Proceedings, COMMAD 6472377, pp. 95-96
- [18] Glicksman, M.: *Phys. Rev.* 111 ,1958, 125.